

Effect of Rapid Solidification and Addition of Cu_3P on the Mechanical Properties of Hypereutectic Al-Si Alloys

Miguel Ángel Suárez-Rosales^a, Raúl Pinto-Segura^b, Elia Guadalupe Palacios-Beas^b, Alfredo Hernández-Herrera^b, José Federico Chávez-Alcalá^{b*}

^a Instituto de Investigaciones en Materiales, Universidad Nacional Autónoma de México – UNAM, México, D.F., México

^b Department of Engineering in Metallurgy and Materials, Escuela Superior de Ingeniería Química e Industrias Extractivas – ESIQIE, Instituto Politécnico Nacional – IPN, México, D.F., México

Received: February 15, 2016; Revised: July 7, 2016; Accepted: July 29, 2016

The combined processes; rapid solidification, addition of Cu_3P compound and heat treatments to improve the mechanical properties of the hypereutectic Al-13Si, Al-20Si and Al-20Si-1.5Fe-0.7Mn alloys (in wt. %) was studied. Optical microscopy and scanning electron microscopy were used to characterize the microstructures. The mechanical properties were evaluated by tensile tests. It was found that the cooling rate (20-50°C/s) used to solidify the alloys plus the addition of Cu_3P compound favored the formation of fine primary Si and the transformation of the Al/Si eutectic from acicular to semi-transformed morphology. The spheroidization of the Al/Si eutectic after heat treatment caused an increase in the elongation (%) compared with the as-cast alloys. Al-13Si alloy showed the highest UTS and elongation (%) values, reaching values up to 215 MPa and 9.6%, respectively. On the other hand, the Al-20Si-1.5Fe-0.7Mn alloy showed the lowest UTS (180MPa) and elongation (3.4%) values. The formation of the Fe-intermetallic compounds caused a negative effect on the mechanical properties of the Al-20Si-1.5Fe-0.7Mn alloy.

Keywords: Aluminum alloys, Semi-rapid solidification, Heat treatment, Microstructure, Mechanical properties

1. Introduction

The hypereutectic Al-Si alloys considered as metal-matrix composites reinforced by hard particles show good wear resistance, low thermal expansion coefficient and high elastic modulus. These properties are attributed to the uniform distribution, size and volume fraction of hard Si particles and in some cases for additional Fe-intermetallic compounds in the soft aluminum matrix¹. These kinds of alloys have been used primarily in the automotive industry and for wear resistant applications. However, their low ductility, insufficient strength, and low fracture toughness impede to extend their applications^{2,3}.

Hypereutectic Al-Si alloys produced by conventional melting techniques exhibit poor mechanical properties. The low cooling rates produce an overgrowth of primary Si in the aluminum matrix as well as a large fraction volume of Al/Si eutectic⁴. These effects result in an increase of fragility and reduction of plasticity of the alloys. To overcome the above mentioned problems and to improve the mechanical properties, several solutions have been proposed such as addition of modifier elements and variation of solidification rates⁵. The addition of phosphorus compounds is one of the best ways to produce fine particles of primary Si with beneficial shape and uniform distribution^{6,8}. The rapid solidification is

another important way to refine not only the primary Si but also the grain size of aluminum matrix and all coexisting phases in the microstructure⁹.

In addition to the solutions described above, the mechanical properties of the as-cast Al-Si alloys can be improved by additional heat treatments that increase the strength of soft matrix and decrease the risk of brittle fracture^{10,11}. The risk of brittle fracture can be reduced by the spheroidization of Al/Si eutectic and by reducing the intensity of the stress-concentration effect on the primary Si particles. Fine as-cast microstructures have shown better response to subsequent heat treatment and also less tendency for low-energy brittle cracking. Therefore, a control of the solidification process to obtain fine microstructures with high dispersion degree of the constituent phases and a subsequent spheroidization heat treatment are required to increase the mechanical properties of the hypereutectic Al-Si alloys. The purpose of the present work is to improve the mechanical properties (elongation % and strength) of the hypereutectic Al-Si alloy using rapid solidification, addition of phosphorous compounds to decrease the size of primary Si, and heat treatments to modify the Al/Si eutectic. Besides, the addition of high Fe content to form Fe-intermetallic compounds was proposed to evaluate their effect on the strength and elongation (%) properties.

* e-mail: jfchavez@ipn.mx

2. Experimental procedures

The hypereutectic Al-13Si, Al-20Si and Al-20Si-1.5Fe-0.7Mn alloys (in wt. %) were fabricated using commercial pure elements (99.9%) in an induction furnace. The melts were degassed with hexachloroethane to reduce the hydrogen level. Besides, the melts were modified using an Al-5Ti-B alloy for grain refinement and Cu_3P (0.15%wt.) compound to modify the size of the primary Si particles.

The alloys were poured into a rectangular copper mold with cooling system (using a constant flow of water). The dimensions of the mold cavity used were 0.12 m long, 0.06 m high and 0.008 m wide.

The chemical composition of the alloys was analyzed by optical emission spectroscopy (OES) on the as-cast ingots. At least 10 measurements were performed on each ingot to determine the average composition. To modify the Al/Si eutectic, the alloys were heat treated for 12h at 540°C in an electric resistance furnace and quenched into an oil container. Subsequently, the alloys were heated at 250°C for 5h and then air-cooled.

Several samples were prepared by standard metallographic techniques for their microstructural analysis. The microstructures were analyzed using optical microscopy (OM) and scanning electron microscopy (SEM). Moreover, punctual SEM-microanalysis was carried out to identify the different phases in the microstructure. Image analyses were performed on approximately 10 micrographs for each alloy to measure the length and area of the primary Si and Fe-intermetallic compounds. From the micrographs of the Al-13Si alloy, the secondary dendrite arm spacing (SDAS) was obtained by measuring the distance between neighboring secondary dendrite arms. For this purpose commercial image analyzer software was used.

In order to estimate the average cooling rate (R) reached by the cooling system, the following empirical equations reported in the literature for Al-Si alloys were used^{12,13}:

$$\log(dT/dt) = -[\log(\text{SDAS}) - 2.37]/0.4 \quad (1)$$

$$\text{SDAS} = 39.4R^{-0.317} \quad (2)$$

where (dT/dt) is the cooling rate (in °C/s) and the constants (39.4 and 0.317) were taken from the literature¹³. The average SDAS values measured in the Al-13Si alloy and in an additional hypoeutectic Al-10Si alloy were used to carry out the calculations.

Rectangular tensile specimens (total length=100mm, width=6.4mm, thickness=6mm and gauge length=25.4mm) were machined from the as-cast and heat treated ingots according to ASTM-E8 standard. All the tensile tests were performed at room temperature using an Instron machine (a 10 ton Shimadzu machine) with a fixed cross head speed of 0.5mm^s⁻¹.

3. Results and Discussion

3.1 Characterization of the as-cast alloys

The experimental chemical compositions of the alloys are shown in Table 1. As can be observed, the results fulfill with the composition raised in this study. Figure 1 shows optical micrographs of the alloys in as-cast condition.

The Al-13Si alloy is near of the eutectic composition (Al-12Si); its microstructure is mainly constituted by Al/Si eutectic with small amounts of primary Si particles and α -dendrites, Figure 1a. On the other hand, the microstructures of the Al-20Si and Al-20Si-1.5Fe-0.7Mn alloys consist of primary Si with polygonal morphology and Al/Si eutectic with needle shape morphology embedded in a α -Al matrix, Figures 1b-c.

The average SDAS values (between 11mm and 15mm) measured in the Al-13Si alloy and in an additional hypoeutectic Al-10Si were used in equations (1) and (2) to estimate the cooling rate reached by the cooling system. No α -dendrites were observed in Al-20Si and Al-20Si-1.5Fe-0.7Mn alloys; therefore, these alloys were not considered for the calculations of R value. According with the aforementioned equations, the alloys were solidified in a cooling rate range from 20 to 50°C/s.

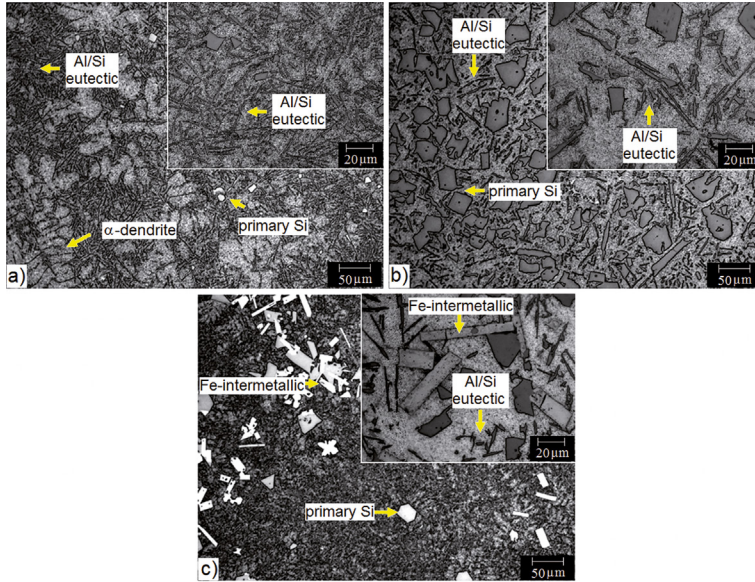
The rapid cooling rate used to solidify the alloys not only caused refining of the different phases of the microstructure but also modification of the Al/Si eutectic (magnification of the eutectics is shown inside of Fig. 1a-c). For instance, the Al/Si eutectic of the Al-13Si alloy seems to be of semi-transformed type (class 3) finely distributed in the α -Al matrix. Regarding to the Al-20Si and Al-20Si-1.5Fe-0.7Mn alloys, the high cooling rate minimized the overgrowth or thickening of the Al/Si eutectic.

The addition of the Cu_3P compound together with the cooling rate used to solidify the alloys caused a significant decrease in the size of primary Si as well as a uniform distribution in the α -Al matrix. The average length and area values of the primary Si obtained in the Al-13Si, Al-20Si and Al-20Si-1.5Fe-0.7Mn alloys, were 9.65 ± 2.5 mm (230 mm²), 29 ± 3 mm (1.25×10^3 mm²) and 26 ± 2.5 mm (1.3×10^3 mm²), respectively.

The average size of primary Si obtained in this study is lower than those reported for the slowly solidified hypereutectic Al-Si alloys and also for alloys solidified under similar cooling rates without the addition of structure refiners^{14, 15}. Comparing the results of the hypereutectic alloys with the same chemical compositions and solidified under similar cooling rates (without the addition of Cu_3P compound), the average length of the primary Si was decreased between 55 and 57%¹⁶.

Table 1: Chemical composition of the hypereutectic Al-Si alloys (in wt.%).

| Alloy | Si | Fe | Mn | Al |
|---------------------|-----------|-----------|--------------|---------|
| Al-13Si | 13.2 ±0.2 | 0.22 ±0.1 | 0.004 ±0.002 | Balance |
| Al-20Si | 20.3 ±0.2 | 0.22 ±0.1 | 0.006 ±0.002 | Balance |
| Al-20Si-1.5Fe-0.7Mn | 20.1 ±0.2 | 1.6 ±0.1 | 0.6±0.002 | Balance |

**Figure 1:** Optical micrographs of the hypereutectic: a) Al-13Si, b) Al-20Si and c) Al-20Si-1.5Fe-0.7Mn alloys in as-cast condition. Inset shows eutectic morphology

The large size of the primary Si contributes to the low ductility of the Al-Si alloys. Other important factor that affects the ductility of the alloys is the Fe content, higher amounts than 0.2% produces Fe-intermetallic compounds¹⁷. In the Al-20Si-1.5Fe-0.7Mn alloy with high Fe content, several types of Fe-intermetallic compounds were formed. Figure 2 shows in detail the size and morphology of these compounds. In order to identify the type of Fe-compound, punctual SEM-EDS microanalysis was carried out on each of them. The small cube-shaped Fe-intermetallic compound shown in Figure 2a, has a composition of $Al_{60.4}Si_{13.1}Fe_{16.5}Mn_{7.1}Cr_{2.9}$, which was identified as the $Al_{15}Si_2MnFe_2$ phase, with sizes of 45-50 nm². The large cube-shaped Fe-compound identified as the $\delta-Al_4FeSi_2$ phase has an average size of 331.5nm² and a chemical composition of $Al_{45.8}Si_{26.3}Fe_{22.6}Mn_{4.2}Ti_{0.4}Cr_{0.7}$ Figure 2b. Another predominant Fe-compound of cross-shaped morphology with an average size of 630 nm² and a chemical composition of $Al_{60.10}Si_{10.75}Fe_{18.89}Mn_{7.47}Cr_{2.78}$ was identified as the $\alpha-Al_{15}(Fe,Mn)_3Si_2$ phase with a considerable amount of Cr dissolved, Figure 2c. The addition of Mn to neutralize the effect of iron on the fragility of the alloys, caused an increase of Mn content in the Fe-intermetallic compounds and the formation of more compact morphologies as the $\alpha-Al_{15}(Fe,Mn)_3Si_2$ compound¹⁸. The overgrowth of these Fe-intermetallic compounds can be detrimental for the mechanical properties.

Figure 2d shows needle-shaped Fe-intermetallic compounds with an average composition of $Al_{59.1}Si_{13.5}Fe_{26.3}Mn_{1.1}$, which were identified as the $\beta-Al_3FeSi$ phase. This Fe-intermetallic compound is finely dispersed throughout the microstructure. In previous studies has been found that the $\beta-Al_3FeSi$ compound can grow up to 1 or more millimeters in slowly cooled Al-Si alloys with high Fe levels¹⁹. However, under the solidification conditions used in this work, these Fe-intermetallic compounds reached sizes between 7.1 µm² and 10.8 µm².

Despite the low Fe content in Al-13Si, Al-20Si alloys, the formation of small proportions and fine scale of the $\beta-Al_3FeSi$ compound was also observed. The $\beta-Al_3FeSi$ compound is particularly harmful to the Al-Si based alloys, the needles/plates morphologies are extremely detrimental to both strength and ductility, its control is essential.

3.2 Characterization of the heat treated alloys

Figure 3 shows the microstructures of the alloys after heat treatment (spheroidization). From the Figure 3a, it can be observed a complete spheroidization of the Al/Si eutectic in the Al-13Si alloy and a high degree of spheroidization in Al-20Si and Al-20Si-1.5Fe-0.7Mn alloys, Figures 3b-c. The high spheroidization degree of the Al/Si eutectic obtained in the Al-13Si alloy can be attributed to the semi-transformed morphology obtained in

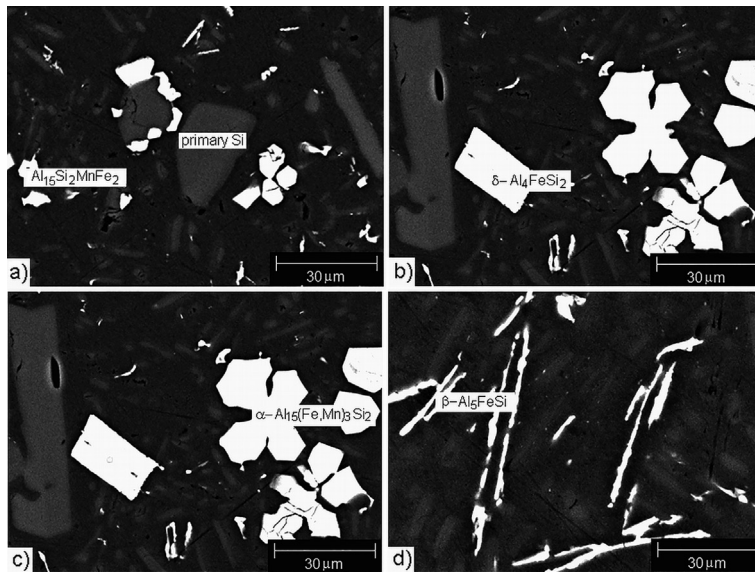


Figure 2: SEM-micrographs of Fe-intermetallic compounds formed in the Al-20Si-1.5Fe-0.7Mn alloy.

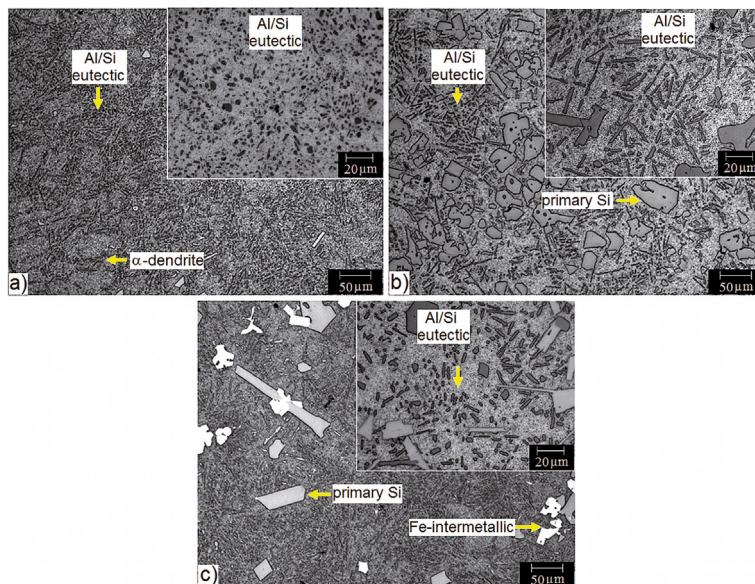


Figure 3: Optical micrographs of the hypereutectic: a) Al-13Si, b) Al-20Si and c) Al-20Si-1.5Fe-0.7Mn alloys after heat treatment. Inset shows spheroidized eutectics.

its as-casting condition. On the other hand, the sharp edges of primary Si formed in Al-20Si and Al-20Si-1.5Fe-0.7Mn alloys were slightly modified to round forms. The morphologies of the Fe-intermetallic compounds remained unchanged. The iron-containing intermetallic phases in Al-Si based alloys are generally largely unaffected by typical T4 or T6 heat treatments²⁰.

3.3 Mechanical properties

The tensile test was carried out to evaluate the degree of modification of the microstructures with a particular interest in the maximum elongation (%) and strength. Figure 4 shows

the stress-strain curves of the alloys in as-cast condition and after heat treatment. Table 2 summarizes the results of the mechanical properties.

For the alloys in as-cast condition, the Al-13Si alloy shows the highest mechanical properties with an ultimate tensile strength (UTS) of 212 ± 2.5 MPa and an elongation to fracture of 6.4%. The Al-20Si alloy with high Si content shows UTS values close to the obtained in Al-13Si alloy but with a lower elongation (%) value. For the Al-20Si-1.5 Fe-0.7Mn alloy with high Si and Fe contents the elongation to fracture and UTS decreased to 2.2% and 182 ± 2.5 MPa, respectively. The UTS obtained in the three alloys are similar

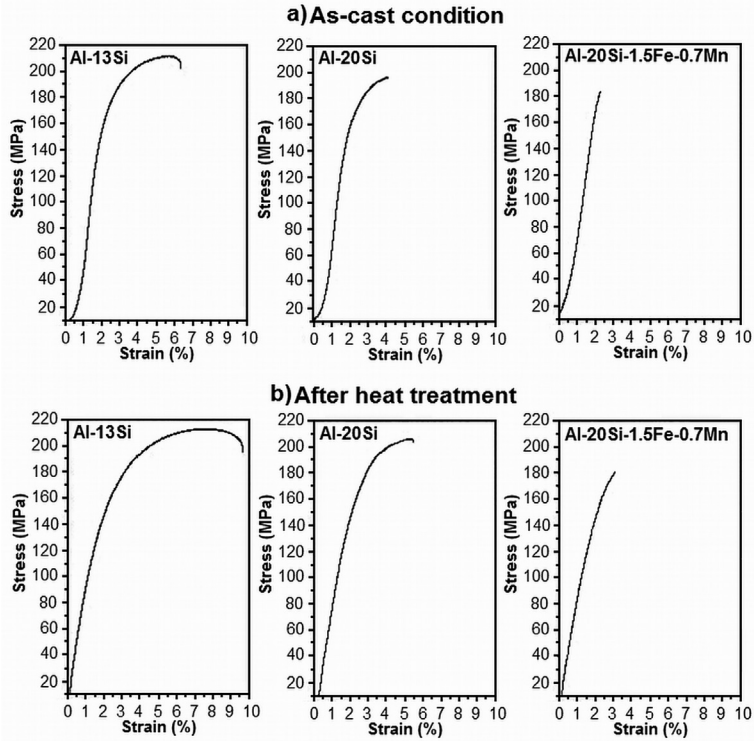


Figure 4: Stress-strain curves of Al-13Si, Al-20Si and Al-20Si-1.5Fe-0.7Mn alloys in a) as-cast condition and b) after heat treatment.

Table 2: Tensile properties of the hypereutectic Al-Si alloys.

| Alloy | Cast condition | | After heat treatment | |
|---------------------|---------------------------------|----------------------------|---------------------------------|----------------------------|
| | Ultimate tensile Strength (MPa) | Elongation to Fracture (%) | Ultimate tensile Strength (MPa) | Elongation to Fracture (%) |
| Al-13Si | 212 ± 2.5 | 6.4 | 215 ± 2.5 | 9.6 |
| Al-20Si | 200 ± 2.5 | 4.2 | 204 ± 2.5 | 5.6 |
| Al-20Si-1.5Fe-0.7Mn | 182 ± 2.5 | 2.2 | 180 ± 2.5 | 3.4 |

than the results reported by Darvishi et al.²¹ and higher than those Al-Si alloys conventionally solidified.

The lower mechanical properties obtained in the Al-20Si-1.5Fe-0.7Mn alloy can be attributed to the high Fe content that produced large amount of coarse Fe-intermetallic compounds in the microstructure. It is well known that the Fe-intermetallic compounds are detrimental to the mechanical properties, since its fracture toughness under tensile load is much lower than that for Al matrix or Si particles. When aluminum alloys contain high iron content, the UTS tend to decrease.

After the heat treatment (spheroidization) the elongation to fracture of the alloys increased, while the UTS values were not modified. The maximum UTS (215 ± 2.5 MPa) and elongation (9.6%) values were obtained in the Al-13Si alloy. On the other hand, the minimum UTS (180 ± 2.5 MPa) and elongation (3.4%) values were obtained in the Al-20Si-1.5Fe-0.7Mn alloy. The mechanical properties obtained in this study are higher than the results reported in a previous work¹⁶. The increase of the

UTS and the elongation (%) values could be attributed to the refinement of the primary Si due to combined effect of rapid solidification and the addition of the phosphorous compound.

The heat treatment increased the elongation in the Al-13Si alloy up to 9.6%. On the other hand, the elongation in Al-20Si-1.5Fe-0.7Mn alloy was increased only 3.4%. The presence of Fe-intermetallic compounds in the microstructure directly affected the ductility of the Al-20Si-1.5Fe-0.7Mn alloy. It is known that coarse silicon particles and the Fe-intermetallic compounds also serve as crack nucleation sites in Al-Si alloys²². The Al-20Si alloy with the same Si content than Al-20Si-1.5Fe-0.7Mn alloy but without Fe content showed higher elongation (%). The reason is that the Fe-intermetallic compounds are detrimental to mechanical properties, because these compounds are much more easily fractured under the tensile load than the primary Si particles or aluminum matrix due to their brittle nature¹⁸.

Figure 5 shows the fractures of the Al-20Si-1.5Fe-0.7Mn alloy in as-cast condition and after heat treatment.

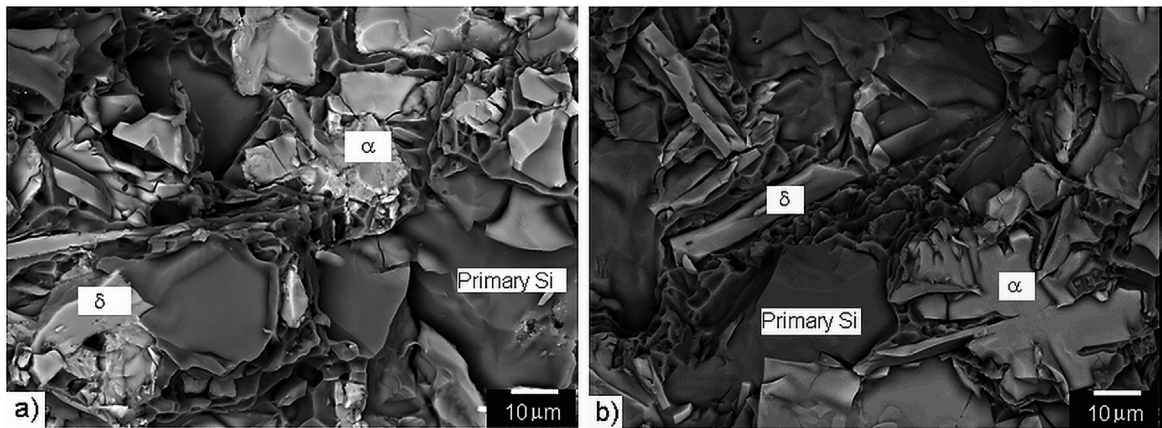


Figure 5: SEM-Images of fractures obtained in Al-20Si-1.5Fe-0.7Mn alloy in a) as cast-condition and b) after heat treatment

Several fractured and fragmented Fe-intermetallic compounds can be observed in the fracture of the as-cast alloy, Figure 5a. The fracture generated in this alloy could be initiated in the Fe-intermetallic compounds and then by the primary Si and finally propagate through the aluminum matrix. Figure 5b shows the fracture of the Al-20Si-1.5Fe-0.7Mn alloy after heat treatment. In this condition, the Fe-intermetallic compounds are not fragmented. However, the elongation (3.4%) obtained in this alloy is lower than the Al-20Si alloy in the same condition. It is thought that the fracture can also be generated by the Fe-intermetallic compounds.

4. Conclusions

The combined effects of rapid solidification, addition of phosphorus compound and heat treatments on the mechanical properties of the hypereutectic Al-Si alloys were analyzed.

The cooling rate (20-50°C/s) used to solidify the alloys favored the formation of fine microstructures and transformation of the Al/Si eutectic from acicular to semi-transformed morphology. The addition of the phosphorous compound plus the rapid solidification caused a decrease of the length and area values of the primary Si, reaching average sizes of 9.65 ± 2.5 mm (230 mm²), 29 ± 3 mm (1.25×10^3 mm²) and 26 ± 2.5 mm (1.3×10^3 mm²) in Al-13Si, Al-20Si and Al-20Si-1.5Fe-0.7Mn alloys, respectively.

After the spheroidization heat treatment the ultimate tensile stress (UTS) values were unchanged while the elongation (%) was increased compared with the as-cast alloys. The Al-13Si alloy showed the highest UTS and percentage of elongation, reaching values up to 215 ± 2.5 MPa and 9.6%, respectively. On the other hand, the Al-20Si-1.5Fe-0.7Mn alloy showed the lowest UTS (180 ± 2.5 MPa) and elongation (3.4%) values. The formation of the Fe-intermetallic compounds restricted the increase of the mechanical properties.

5. Acknowledgements

The authors acknowledge the financial support from Consejo Nacional de Ciencia y Tecnología (CONACYT) and SIP-IPN.

6. References

- Vijayan V, Narayan Prabhu K. Review of microstructure evolution in hypereutectic Al-Si alloys and its effect on wear properties. *Transactions of the Indian Institute of Metals*. 2014;67(1):1-18.
- Basavakumar KG, Mukunda PG, Chakraborty M. Impact toughness in Al-12Si and Al-12Si-3Cu cast alloys-Part 1: Effect of process variables and microstructure. *International Journal of Impact Engineering*. 2008;35(4):199-205.
- Ma A, Suzuki K, Saito N, Nishida Y, Takagi M, Shigematsu I, et al. Impact toughness of an ingot hypereutectic Al-23 mass% Si alloy improved by rotary-die equal-channel angular pressing. *Materials Science & Engineering: A*. 2005;399(1-2):181-189.
- Abu-Dheir N, Khraisheh M, Saito K, Male A. Silicon morphology modification in the eutectic Al-Si alloy using mechanical mold vibration. hypereutectic Al-23 mass% Si alloy improved by rotary-die equal-channel angular pressing. *Materials Science & Engineering: A*. 2005;393(1-2):109-117.
- Channappagoudar S, Sannayallappa N, Desai V, Karodi V. Influence of combined grain refinement and modification on the microstructure, tensile strength and wear properties of Al-15Si, Al-15Si-4.5Cu alloys. *International Journal of Materials Research*. 2015;106(9):962-969.
- Xu CL, Wang HY, Yang YF, Jiang QC. Effect of Al-P-Ti-TiC-Nd₂O₃ modifier on the microstructure and mechanical properties of hypereutectic Al-20 wt.%Si alloy. *Materials Science & Engineering: A*. 2007;452-453:341-346.
- Zuo M, Zhao D, Teng X, Geng H, Zhang Z. Effect of P and Sr complex modification on Si phase in hypereutectic Al-30Si alloys. *Materials & Design*. 2013;47:857-864.

8. Angadi BM, Chennakesava Reddy A, Katti VV, Nagathan VV, Kori SA. Effect of phosphorous, titanium-boron and titanium on thermal properties of hypereutectic aluminium-silicon alloys. *International Journal of Applied Engineering Research*. 2015;10(23):43752-43757.
9. Uzun O, Yılmaz F, Kölemen U, Başman N. Sb effect on micro structural and mechanical properties of rapidly solidified Al-12Si alloy. *Journal of Alloys and Compounds*. 2011;509(1):21-26.
10. Peng J, Tang X, He J, Xu D. Effect of heat treatment on microstructure and tensile properties of A356 alloys. *Transactions of Nonferrous Metals Society of China*. 2011;21:1950-1956.
11. Ogris E, Wahlen A, Lüchinger H, Uggowitzer PJ. On the silicon spheroidization in Al-Si alloys. *Journal of Light Metals*. 2002;2(4):263-269.
12. Drouzy M, Richard M. Effet des conditions de solidification sur la qualité des alliages de fonderie de A-U5 G T et A-S7 G, estimation des caractéristiques mécaniques. *Founderie*. 1969;285:49-56.
13. Chen R, Shi Y, Xu Q, Liu B. Effect of cooling rate on solidification parameters and microstructure of Al-7Si-0.3Mg-0.15Fe alloy. *Transactions of Nonferrous Metals Society of China*. 2014;24:1645-1652.
14. Choi YS, Lee JS, Kim WT, Ra HY. Solidification behavior of Al-Si-Fe alloys and phase transformation of metastable intermetallic compound by heat treatment. *Journal of Materials Science*. 1999;34(9):2163-2168.
15. Kotadia HR, Das A. Modification of solidification microstructure in hypo- and hyper-eutectic Al-Si alloys under high-intensity ultrasonic irradiation. *Journal of Alloys and Compounds*. 2015;620:1-4.
16. Suarez MA, Figueroa I, Cruz A, Hernandez A, Chavez JF. Study of the Al-Si-X system by different cooling rates and heat treatment. *Materials Research*. 2012;15(5):763-769.
17. Khalifa W, Samuel FH, Gruzleski JE. Iron intermetallic phases in the Al corner of the Al-Si-Fe system. *Metallurgical and Materials Transactions A*. 2003;34(3):807-825.
18. Hwang JY, Doty HW, Kaufman MJ. The effect of Mn additions on the microstructure and mechanical properties of Al-Si-Cu casting alloys. *Materials Science and Engineering: A*. 2008;488(1-2):496-504.
19. Moustafa MA. Effect of iron content on the formation of β -Al₃FeSi and porosity in Al-Si eutectic alloys. *Journal of Materials Processing Technology*. 2009;209(1):605-610.
20. Taylor JA. Iron-Containing Intermetallic Phases in Al-Si Based Casting Alloys. *Procedia Materials Science*. 2012;1:19-33.
21. Darvishi A, Maleki A, Atabaki MM, Zargami M. The mutual effect of iron and manganese on microstructure and mechanical properties of aluminum-silicon alloy. *Metallurgical and Materials Engineering*. 2010;16(1):11-24.
22. Zhou J, Duszczek J. Fracture features of a silicon-dispersed aluminium alloy extruded from rapidly solidified powder. *Journal of Materials Science*. 1990;25(10):4541-4548.